Pergamon

Int. J. Heat Mass Transfer. Vol. 38, No. 16, pp. 2997–3004, 1995

0017–9310/95 $9.50+0.00

0017–9310(95)00045–3

Optimal allocation of a heat-exchanger inventory in heat driven refrigerators

A. BEJAN and J. V. C. VARGAS

Department of Mechanical Engineering and Materials Science, Duke University, Durham, NC 27708-0300, U.S.A.

and

M. SOKOLOV

Department of Fluid Mechanics and Heat Transfer, Tel-Aviv University, Ramat-Aviv 69978, Israel

(*Received* 13 *June* 1994 *and in final form* 12 *January* 1995)

Abstract—This paper reports the thermodynamic optimization (or entropy generation minimization) of a heat-driven refrigeration plant, that is, a refrigerator without work input, which is driven by a heat source. The treatment accounts for the heat transfer irreversibilities of the three heat exchangers, and for the finiteness of the total heat-exchanger inventory. The operating conditions for maximum refrigeration rate are determined. It is shown that the heat-exchanger inventory must be divided optimally between the three heat exchangers. For example, half of the inventory must be placed in the heat exchanger used to reject heat to the ambient. The maximum refrigeration rate per unit of total heat exchanger inventory is reported. These thermodynamic optimization principles are then applied to a refrigerator driven by heat transfer from a solar collector.

1. INTRODUCTION

The method of entropy generation minimization has emerged during the last two decades as a distinct subfield in heat transfer (e.g. refs. [1, 2]). The method consists of the simultaneous application of heat transfer and thermodynamics principles in the pursuit of realistic models of heat transfer processes, devices and installations. By 'realistic' models we mean models that account for the inherent irreversibility of heat, mass and fluid flow processes. In engineering, the entropy generation minimization method is also known as thermodynamic optimization and thermodynamic design.

The importance and growth of this field are further illustrated by the emergence of a parallel activity in physics. The physics work is usually referred to as thermodynamics in finite time (e.g. ref. [3]), and its methodology is the same combination of heat transfer and thermodynamics. Some of the most fundamental results refer to the optimization of power plants and refrigeration plants with heat transfer irreversibilities. In the power generation area, the focus has been on the regime for the production of maximum instantaneous power [4–7], which is equivalent to the regime of minimum entropy generation rate (cf. the Gouy-Stodola theorem, ref. [1], p. 24).

In the refrigeration area, the models that have been optimized based on this method had power input and heat rejection to the ambient [8], as in the case of the vapor compression cycle [9]. They were optimized by maximizing the refrigeration load (rate of heat extraction from the cold space), which is the same as minimizing the rate of entropy generation of the refrigeration plant.

In this paper we apply the method of thermodynamic optimization to a distinct class of refrigeration plants: heat driven refrigeration plants, or plants without work input (Fig. 1, left). Examples of such plants are absorption refrigerators (e.g. ref. [10]), and jet ejector refrigerators (e.g. ref. [11]). Our objectives are to determine:

1. The operating conditions for maximum refrigeration effect, and
2. The optimal way of dividing a finite supply of heat exchanger surface between the three heat exchangers of the refrigeration plant.

Heat driven refrigerators constitute an important class, fundamentally, because of the peculiarity of almost no work input, and, practically, because the driving heat transfer (Q_H in Fig. 1) can be low-grade heat (e.g. solar [12]) or waste heat. The utilization of low-grade heat sources is stressed by environmental and economic considerations. For this reason we conclude the paper with an application of the present method to the optimization of a refrigerator driven by heat transfer from a solar collector.

NOMENCLATURE

a, b	constants
A	heat transfer area
A_C	collector area
B	dimensionless group, equation (35)
G_T	irradiance on collector surface
p_H	price of heat input
p_L	price of refrigeration load
P	profit function, equation (26)
Q_H	heat input
Q_L	refrigeration load
Q_0	condenser heat transfer
T_H	generator temperature
T_L	refrigeration load temperature
T_{st}	collector stagnation temperature
T_0	ambient temperature
U	overall heat transfer coefficient based on A
W	power output
x	conductance fraction, equation (19)
y	conductance fraction, equation (29)
z	conductance fraction, equation (29).

Greek symbols

τ	dimensionless temperature, T/T_0.

Subscripts and superscripts

$()_C$	Carnot (reversible) compartment
$()_H$	generator, or solar collector
$()_L$	evaporator
$()_{max}$	maximum
$()_{opt}$	optimum
$()_P$, $()^P$	power plant part
$()_R$, $()^R$	refrigeration plant part
$()_0$	ambient
$(\tilde{\ })$	dimensionless variable.

2. MODEL WITH THREE HEAT TRANSFER IRREVERSIBILITIES

The main external features of a heat driven refrigerator are shown on the left side of Fig. 1. The working fluid executes cycles while removing the refrigeration load Q_L from the refrigerated space T_L, and rejecting the heat transfer Q_0 to the ambient T_0. The cycle is driven by the heat transfer Q_H received from the source temperature T_H. There is no work transfer between the refrigerator and its environment.

From the outset, we recognize that the refrigerator operates irreversibly because of several entropy-generating mechanisms that are always present, for example, heat transfer, throttling and mixing [11]. In the model shown on the right side of Fig. 1, we have divided the refrigerator into four compartments, the three heat exchangers (Q_H, Q_0, Q_L) and the rest. The heat exchangers account for the irreversibility of the machine, and the remaining components (labeled (C)) are modeled as irreversibility free. In other words, in the following analysis we neglect the irreversibility associated with frictional pressure drops, throttling and mixing. This assumption is consistent with the thermodynamics treatment of power plants [4–7, 13] and refrigeration plants based on the vapor compression cycle [9].

The four compartments of the irreversible refriger-

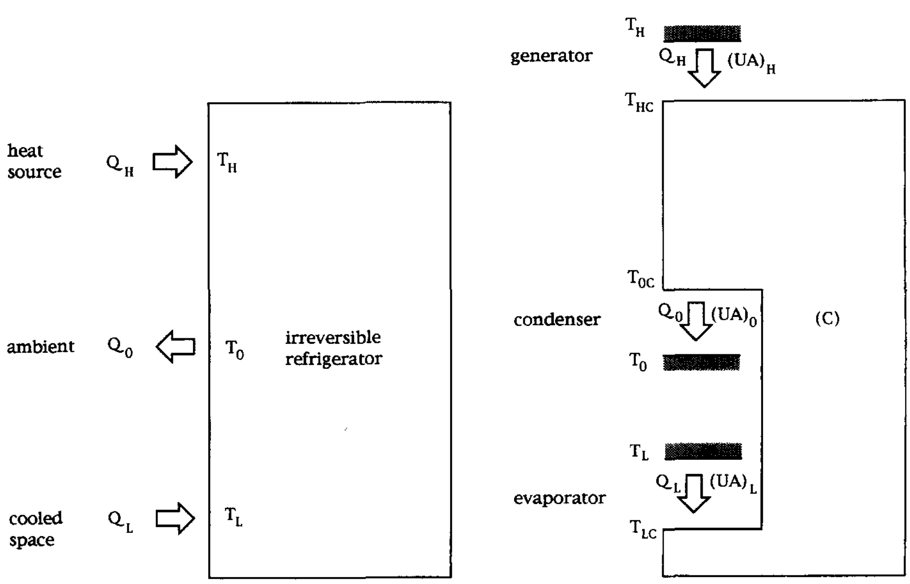

Fig. 1. Model with heat transfer irreversibilities (right) for an irreversible heat-driven refrigerator (left).

ator model are described analytically by the four statements:

$$Q_H = (UA)_H(T_H - T_{HC}) \quad (1)$$

$$Q_0 = (UA)_0(T_{0C} - T_0) \quad (2)$$

$$Q_L = (UA)_L(T_L - T_{LC}) \quad (3)$$

$$\frac{Q_H}{T_{HC}} + \frac{Q_L}{T_{LC}} = \frac{Q_0}{T_{0C}}. \quad (4)$$

In adition, the first law of thermodynamics requires that

$$Q_H + Q_L = Q_0. \quad (5)$$

Each factor of type UA in equations (1)–(3) represents the overall thermal conductance of the respective heat exchanger, or the product between the heat transfer area A and the overall heat transfer coefficient U based on A. The thermal conductances $(UA)_H$, $(UA)_0$ and $(UA)_L$ are rough measures of the sizes (amounts of hardware) of the three heat exchangers, therefore a reasonable economic constraint is [13, 14]

$$UA = (UA)_H + (UA)_0 + (UA)_L, \quad \text{(constant)} \quad (6)$$

which states that the total thermal conductance inventory UA is fixed.

The question on which we focus in the following analysis is how to divide the UA inventory between $(UA)_H$, $(UA)_0$ and $(UA)_L$, such that the refrigeration rate Q_L is maximized. This problem can be solved in several ways. One way is to use the system (1)–(5) to express Q_L as a function of the thermal conductance distribution ratios $(UA)_H/UA$ and $(UA)_L/UA$, and to maximize Q_L with respect to these two degrees of freedom. This approach seems direct; however, the double maximization of Q_L must be performed numerically and the competition between the three irreversibilities is hidden from view. Much more instructive is the alternative method shown next, which is based on conclusions known from the optimization of simpler power and refrigeration plants and takes us close to the final answer by using pure analysis.

3. COUPLED REFRIGERATION AND POWER PLANTS

The absorption refrigeration plant of Fig. 1 (right) is equivalent to the coupling of a power plant and refrigeration plant, as is shown in Fig. 2. The power output (W) from the power plant (P) drives the refrigeration plant (R). The spaces labeled (P) and (R) are irreversibility free. The heat rejection to the ambient, which in Fig. 1 was accommodated by a single heat exchanger, $(UA)_0$, is now effected by two heat exchangers operating in parallel, $(UA)_0^P$ and $(UA)_0^R$. The equivalence between Figs. 1 and 2 is assured by writing

$$Q_0 = Q_0^P + Q_0^R \quad (7)$$

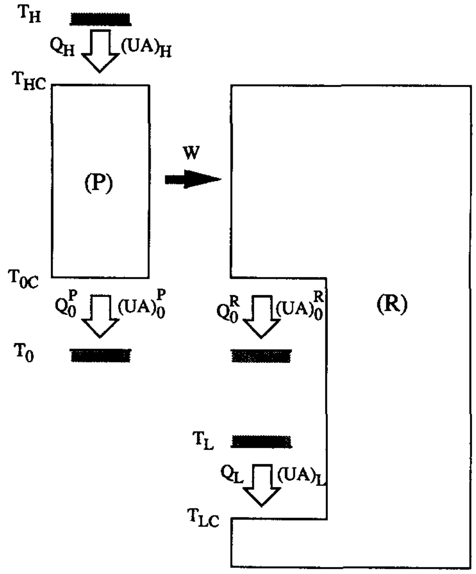

Fig. 2. The model of Fig. 1 (right) as the coupling of a heat transfer-irreversible power plant (P) with a heat transfer-irreversible refrigeration plant (R).

$$(UA)_0 = (UA)_0^P + (UA)_0^R. \quad (8)$$

The power plant portion of the Fig. 2 model has been optimized in refs. [13, 14], in which the instantaneous power output W was maximized with respect to two degrees of freedom (T_{HC} and T_{0C}, or T_{HC}/T_{0C} and $(UA)_H/(UA)_0^P$). The results that are relevant to the present study are

$$(UA)_{H,opt} = (UA)_{0,opt}^P \quad (9)$$

$$W_{max} = \tfrac{1}{4}(UA)_P T_0(\tau_H^{1/2} - 1) \quad (10)$$

where $(UA)_P$ is the total thermal conductance inventory of the power-plant portion (P),

$$(UA)_P = (UA)_H + (UA)_0^P \quad (11)$$

and

$$\tau_H = \frac{T_H}{T_0} > 1. \quad (12)$$

Equation (9) states that $(UA)_P$ must be divided equally between the two heat exchangers of the power-plant portion. The question that remains is how much of the total inventory UA (Fig. 1) should be allocated to $(UA)_P$.

Similar progress has been made in connection with the refrigerator portion (R) of the model of Fig. 2. Without repeating the analysis of refs. [8] and [15], we know that when W is given the refrigeration load Q_L is maximized if

$$(UA)_{0,opt}^R = (UA)_{L,opt} \quad (13)$$

while the total thermal conductance inventory of the refrigerator portion is constrained,

$$(UA)_R = (UA)_0^R + (UA)_L. \quad (14)$$

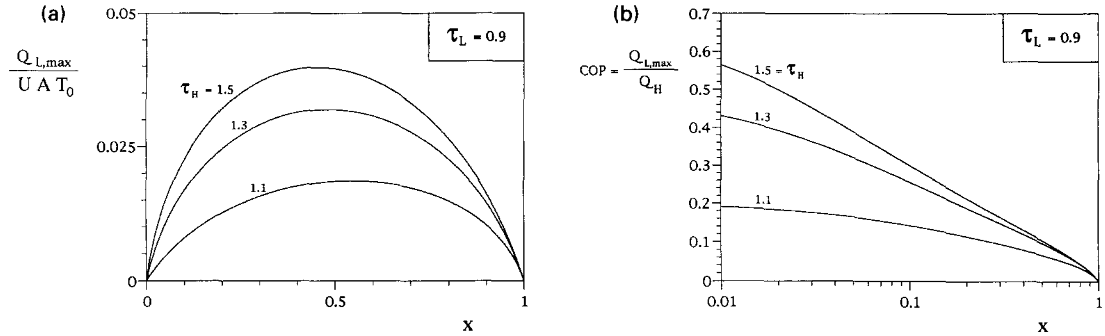

Fig. 3. (a) The maximization of the refrigeration load with respect to the conductance allocation ratio x. (b) The effect of x on the coefficient of performance.

By repeating the analysis presented in ref. [8], it can be shown that the maximum Q_L that corresponds to the optimization rule (13) is

$$Q_{L,max} = \tfrac{1}{8}(UA)_R T_0\{[(4\tilde{W}-\tau_L+1)^2+16\tau_L\tilde{W}]^{1/2} - 4\tilde{W}+\tau_L-1\} \quad (15)$$

where

$$\tau_L = \frac{T_L}{T_0} < 1 \quad (16)$$

$$\tilde{W} = \frac{W}{(UA)_R T_0}. \quad (17)$$

We now return to the original problem formulated in Fig. 1, by coupling the optimized (P) and (R) portions of Fig. 2. This amounts to setting $W = W_{max}$ in equations (15) and (17), for which W_{max} is given by equation (10). The total thermal conductance inventory UA of the entire installation, equation (6), can be written also in terms of the total inventories of the (P) and (R) portions,

$$UA = (UA)_P + (UA)_R, \quad \text{(constant)} \quad (18)$$

or by introducing the fraction x

$$x = \frac{(UA)_P}{UA}, \quad 1-x = \frac{(UA)_R}{UA}. \quad (19)$$

After these substitutions, equation (15) becomes

$$\frac{Q_{L,max}}{UAT_0} = \tfrac{1}{8}(1-x)\{[(4\tilde{W}_{max}-\tau_L+1)^2+16\tau_L\tilde{W}_{max}]^{1/2} - 4\tilde{W}_{max}+\tau_L-1\} \quad (20)$$

where

$$\tilde{W}_{max} = \frac{x(\tau_H^{1/2}-1)}{4(1-x)}. \quad (21)$$

The expression listed in equation (20) has been maximized numerically with respect to x, while holding the external temperature ratios τ_H and τ_L fixed. The procedure is illustrated in Fig. 3(a). It is interesting to point out that during this maximization the coefficient of performance $COP = Q_{L,max}/Q_H$ does not exhibit a maximum with respect to x, Fig. 3(b). The reason is that τ_H is assumed fixed, the heat input Q_H is limitless and the only restriction is size and allocation of the UA inventory.

The optimal allocation fraction $x_{opt}(\tau_H, \tau_L)$ obtained based on Fig. 3(a) is shown in Fig. 4. The answer sought in connection with equation (6) is now complete: it is contained in Fig. 4 and equations (9) and (13). In conclusion, the optimal three-way allocation of UA between the generator, condenser and evaporator is

$$(UA)_{H,opt} = \tfrac{1}{2}x_{opt}UA \quad (22)$$

$$(UA)_{0,opt} = \tfrac{1}{2}UA \quad (23)$$

$$(UA)_{L,opt} = \tfrac{1}{2}(1-x_{opt})UA. \quad (24)$$

It is interesting that the optimal condenser always demands half of the total thermal conductance inventory, regardless of the temperature ratios T_H/T_0 and T_L/T_0. Figure 4 shows that when T_L/T_0 is not much smaller than 1, the ratio x_{opt} is equal to roughly $\frac{1}{2}$. This means that the optimal generator and evaporator conductances must have approximately the same size,

$$(UA)_{H,opt} \simeq (UA)_{L,opt} \simeq \tfrac{1}{4}UA. \quad (25)$$

Figure 5 shows the maximum refrigeration rate that corresponds to the optimal allocation of the UA inventory (equations (22)–(24) and Fig. 4). The dimensionless group listed on the ordinate is a reminder that

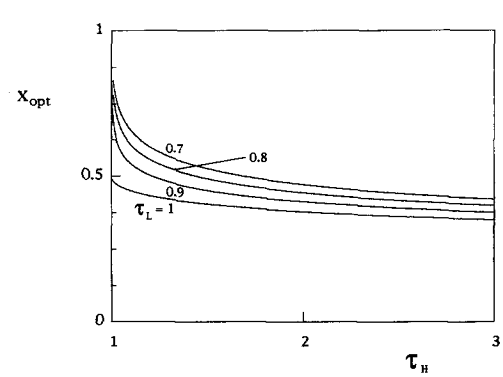

Fig. 4. The optimal thermal conductance allocation ratio $x = (UA)_P/UA$.

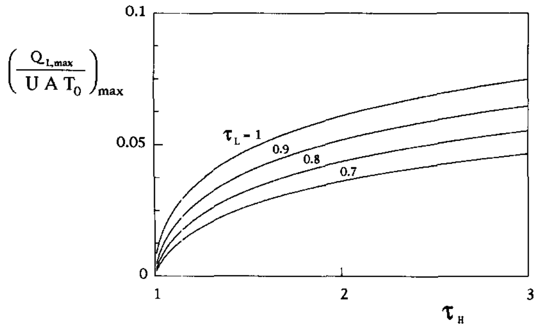

Fig. 5. The maximum refrigeration rate of a heat driven refrigerator with fixed thermal conductance.

Q_L has been maximized twice, first based on equation (13), and, second, by using x_{opt}. The resulting Q_L maximum increases monotonically with the heat source temperature τ_H, and decreases monotonically as the refrigeration load temperature τ_L decreases.

4. THE EFFECT OF THE COST OF THE HEAT INPUT

The optimization described so far was based on maximizing the refrigeration load Q_L. This choice is appropriate only when the cost of the heat input Q_H is negligible when compared with the economic value of the refrigeration effect Q_L. In general, however, the heat input is not available freely, and the relevant objective function to maximize is the profit

$$P = p_L Q_L - p_H Q_H \tag{26}$$

Here p_L and p_H are the known prices of the refrigeration load and the heat input. We are interested in dividing the total UA inventory of equation (6) such that P is maximized.

The maximization of P can be performed numerically, and our results are shown in Figs. 6(a)–(c). The problem statement consists of equations (1)–(6) and (26). We first non-dimensionalized these equations using equations (12) and (16) and

$$\tau_{HC} = \frac{T_{HC}}{T_0}, \quad \tau_{0C} = \frac{T_{0C}}{T_0}, \quad \tau_{LC} = \frac{T_{LC}}{T_0} \tag{27}$$

$$\tilde{Q}_H = \frac{Q_H}{UAT_0}, \quad \tilde{Q}_0 = \frac{Q_0}{UAT_0}, \quad \tilde{Q}_L = \frac{Q_L}{UAT_0}. \tag{28}$$

For brevity, we omit the resulting dimensionless equations, and note that equations (1)–(6) deliver $\tilde{Q}_L$ as a function of five dimensionless numbers, $\tilde{Q}_H$, τ_H, τ_L, y and z, where

$$y = \frac{(UA)_H}{UA}, \quad z = \frac{(UA)_L}{UA}. \tag{29}$$

Note also that according to the UA constraint (6), the equipment fraction allocated to the condenser is

$$\frac{(UA)_0}{UA} = 1 - y - z. \tag{30}$$

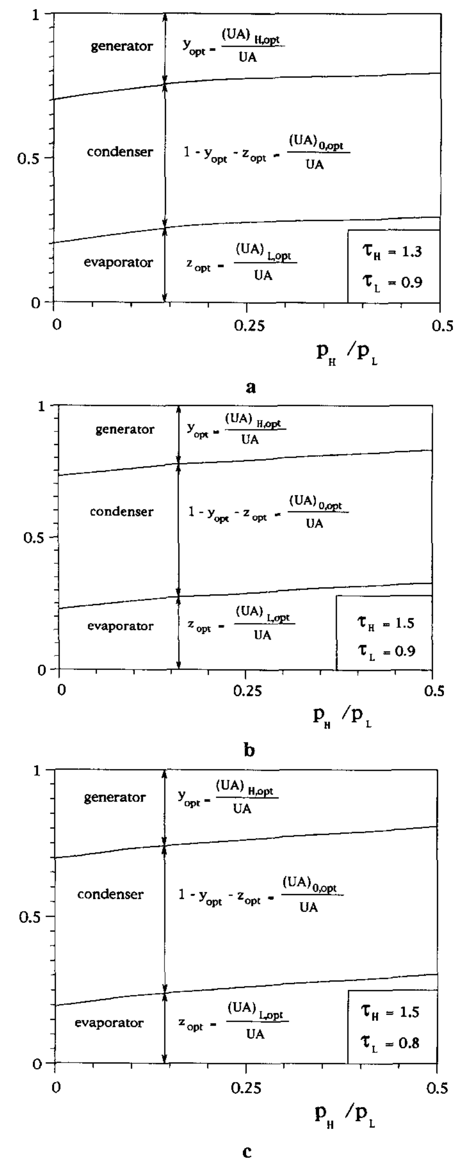

Fig. 6. The effect of the price ratio p_H/p_L on the optimal allocation of thermal conductance between the three heat exchangers.

In conclusion, the non-dimensionalized profit function

$$\tilde{P} = \frac{P}{p_L UAT_0} = \tilde{Q}_L - \frac{p_H}{p_L}\tilde{Q}_H \tag{31}$$

depends on $\tilde{Q}_H$, τ_H, τ_L, y, z and p_H/p_L. We maximized $\tilde{P}$ numerically by varying y and z while holding $\tilde{Q}_H$, τ_H, τ_L and p_H/p_L constant. The pair of optimal values (y_{opt}, z_{opt}) that maximizes $\tilde{P}$ is reported in Figs. 6(a)–(c) for several combinations of $\tilde{Q}_H$, τ_H, τ_L and p_H/p_L. Note that the limit $p_H/p_L = 0$ represents the Q_L maximization results described in the preceding section.

In ejector refrigeration cycle applications the source temperature T_H varies between 80 °C and 130 °C, and the refrigeration load is extracted from temperatures

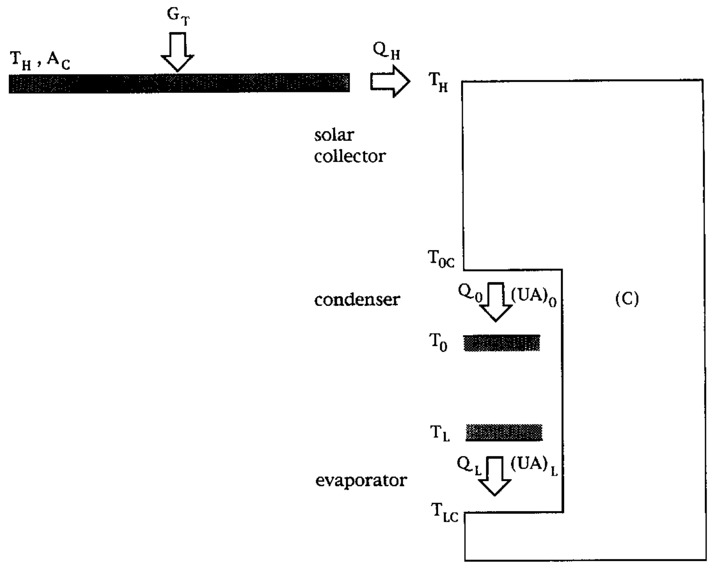

Fig. 7. Refrigerator driven by heat transfer from a solar collector.

T_L ranging from -15 °C to 5 °C [11]. These ranges are represented approximately by $\tau_H = 1.3$ and $\tau_L = 0.9$, which have been used to develop the numerical results shown in Fig. 6(a). The graph shows y_{opt} and z_{opt} in a way that illustrates the splitting of the total thermal conductance (an amount equal to 1 on the ordinate) between the generator, condenser and evaporator.

The most striking feature is that the condenser demands half of the total thermal conductance, regardless of the price ratio p_H/p_L and the external temperature levels (τ_H, τ_L). In other words, the conclusion reached in (23) is more general than in the model of Section 3. In each frame of Fig. 6 we see that $(UA)_{L,opt}$ increases at the expense of $(UA)_{H,opt}$ as the price ratio p_H/p_L increases.

Comparing Figs. 6(a) and (b) we learn that when τ_H increases, the evaporator conductance must be increased, again, at the expense of the generator conductance. Figures 6(b) and (c) show that as τ_L decreases from 0.9 to 0.8 it has a negligible effect on the conductance allocation fractions y_{opt} and z_{opt}.

5. THE OPTIMAL COUPLING BETWEEN THE REFRIGERATOR AND A SOLAR COLLECTOR

Consider now the class of applications where the heat input Q_H is provided at the temperature level T_H by a flat plate solar collector, Fig. 7. The relation between Q_H and the collector temperature T_H can be expressed as

$$Q_H = A_C G_T[a-b(T_H-T_0)] \tag{32}$$

where A_C is the collector area, G_T is the irradiance at the collector surface, and a and b are two constants that can be calculated as shown by Sokolov and Hershgal [12]. Equation (32) represents a collector with partial heat loss to the ambient. The group $[a-b(T_H-T_0)]$ is known as the collector efficiency, and

$$T_{st} = T_0 + \frac{a}{b} \tag{33}$$

is the stagnation (i.e. the ceiling) temperature of the collector. When $T_H = T_{st}$ the heat input Q_H is zero.

Sokolov and Hershgal [12] demonstrated that when the collector and heat exchanger are specified, there exists an optimal collector temperature for maximum refrigeration effect, i.e. an optimal *coupling* between the solar collector and the refrigerator. In this section we examine how this coupling is affected by the sizes of the heat exchangers. We begin with the observation that equation (32) replaces equation (1) of the earlier model, and that the collector (A_C, G_T) replaces the generator $(UA)_H$. The solar-driven refrigerator continues to be described by the right side of Fig. 1, for which Q_H is given by equation (32), and the total UA inventory is to be shared by the condenser and the evaporator,

$$UA = (UA)_0 + (UA)_L. \tag{34}$$

The operation of the refrigerator is governed by equations (2)–(5), (32) and (34). These can be restated in dimensionless terms by using τ_{0C}, τ_{LC}, $\tilde{Q}_H$, $\tilde{Q}_0$ and $\tilde{Q}_L$ defined in equations (27) and (28), and the additional parameters

$$\tau_{st} = \frac{T_{st}}{T_0} \quad B = \frac{bA_C G_T}{UA}. \tag{35}$$

We continue to use the evaporator conductance allocation ratio $z = (UA)_L/UA$, and note that this time $(UA)_0/UA = 1-z$. The B parameter describes the size of the collector relative to the cumulative size of the condenser and the evaporator. By solving equations

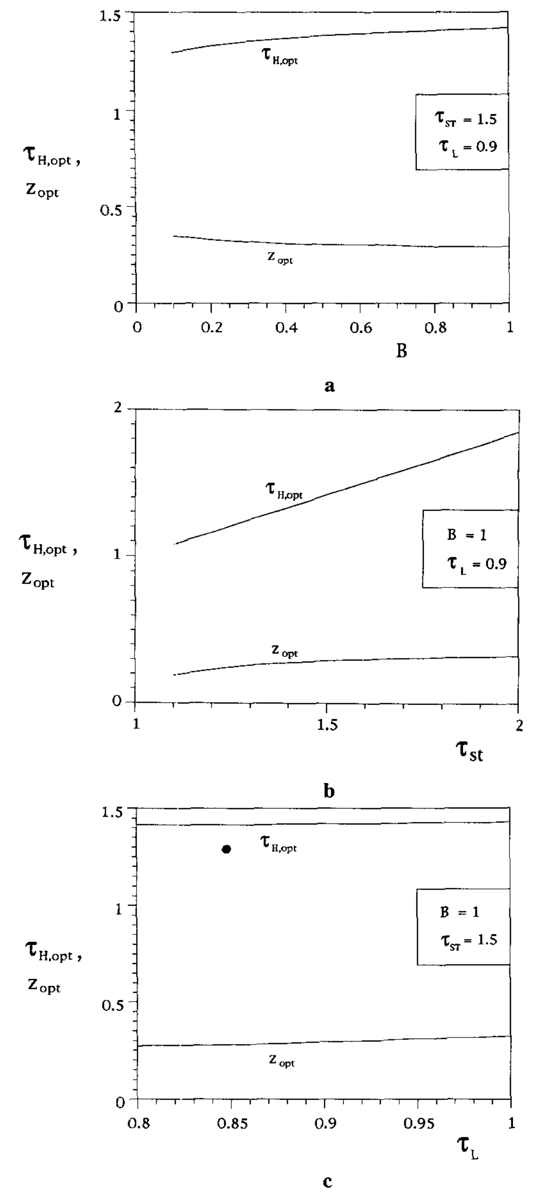

Fig. 8. The optimal collector temperature ($\tau_{H,opt}$) and thermal conductance allocation ratio (z_{opt}). (a) The effect of the collector size (B); (b) the effect of the stagnation temperature (τ_{st}); (c) the effect of the refrigeration temperature (τ_L).

(2)–(5) and (32) numerically, we were able to determine $\tilde{Q}_L$ for a given set of values for B, τ_H, τ_L, τ_{st} and z. We varied τ_H and z until we located the pair ($\tau_{H,opt}$, z_{opt}) that maximizes $\tilde{Q}_L$. The resulting $\tau_{H,opt}$ and z_{opt} values are functions of three parameters, B, τ_{st} and τ_L.

Figure 8(a) shows the effect of the collector size (B) on the optimal collector temperature and thermal conductance allocation ratio. We see that the collector temperature increases only slightly as the B parameter increases by a factor of 10 (from 0.1 to 1). The B effect on z_{opt} is even weaker: in the B range of Fig. 8, z_{opt} is such that the optimal evaporator conductance $(UA)_L$ is roughly one third of the total conductance UA, or about half of the condenser conductance $(UA)_0$. This conclusion agrees approximately with the relative size $(UA)_{L,opt}/(UA)_{0,opt} \simeq \frac{1}{2}$ described by equations (23) and (24).

The effect of the stagnation temperature is illustrated in Fig. 8(b). Both $\tau_{H,opt}$ and z_{opt} increase as τ_{st} increases. Worth noting is that $\tau_{H,opt}$ is consistently greater than $\tau_{st}^{1/2}$, i.e. greater than the optimal collector temperature determined in ref. [16] for a collector coupled to a power cycle that has no heat transfer irreversibilities. Finally, Fig. 8(c) shows that the refrigeration temperature τ_L has an insignificant effect on the optimal results determined in this section.

6. CONCLUSION

In this paper we presented the thermodynamic optimization of heat driven refrigeration plants. This was based on a model (Fig. 1) that accounted for the irreversibility of the plant and the finiteness of the heat exchanger inventory (total thermal conductance). We determined the operating regime for maximum refrigeration effect, and saw how the optimal performance is affected by the extreme temperature levels of the refrigeration plant (Fig. 5).

From a practical standpoint, the most important conclusion is that the maximum refrigeration regime requires that the thermal conductance be allocated in a certain way between the three heat exchangers (Fig. 4). The allocation of the thermal conductance is influenced to some extent by the relative price of the heat source (Fig. 6). The optimal thermal conductance of the ambient-temperature heat exchanger is half of the total supply, and is independent of the relative price of the heat source. The example of the solar driven refrigerator (Section 5) showed that the basic thermodynamic optimization principles developed in the first part of the paper can be used to optimize actual refrigeration plants that are driven by heat transfer.

Acknowledgement—This work was supported by Duke University, Conselho Nacional de Desenvolvimento Cientifico e Tecnologico-CNPq (Brazil), Tel Aviv University, and a travel grant from Ministry of Science and Arts of Israel. Preliminary reports of this international collaborative work were given in refs. [17, 18].

REFERENCES

1. A. Bejan, *Entropy Generation through Heat and Fluid Flow*. Wiley, New York (1982).
2. A. Bejan, The thermodynamic design of heat and mass transfer processes and devices, *Int. J. Heat Fluid Flow*, **8**, 258–276 (1987).
3. B. Andersen, P. Salamon and R. S. Berry, Thermodynamics in finite time, *Phys. Today* September, 62–70 (1984).
4. I. I. Novikov, The efficiency of atomic power stations, *J. Nuclear Energy II* **7**, 125–128 (1958); from *Atomnaya Energiya* **3**(11), 409 (1957).
5. M. M. El-Wakil, *Nuclear Power Engineering*, pp. 162–165. McGraw-Hill, New York (1962).
6. M. M. El-Wakil, *Nuclear Energy Conversion*, pp. 31–35. International Textbook Company, Scranton, PA (1971).
7. F. L. Curzon and B. Ahlborn, Efficiency of a Carnot

engine at maximum power output, *Am. J. Phys.* **43,** 22–24 (1975).
8. A. Bejan, Theory of heat transfer-irreversible refrigeration plants, *Int. J. Heat Mass Transfer* **32,** 1631–1639 (1989).
9. S. A. Klein, Design considerations for refrigeration cycles, *Int. J. Refrig.* **15,** 181–185 (1992).
10. H. Perez-Blanco, Conceptual design of a high-efficiency absorption cooling cycle, *Int. J. Refrig.* **16,** 429–433 (1993).
11. M. Sokolov and D. Hershgal, Operational envelope and performance curves for a compression-enhanced ejector refrigeration system, *ASHRAE Trans.* **97,** 394–402 (1991).
12. M. Sokolov and D. Hershgal, Optimal coupling and feasibility of a solar-powered year-round ejector air conditioner, *Solar Energy* **50,** 507–516 (1993).
13. A. Bejan, *Advanced Engineering Thermodynamics.* Wiley, New York (1988).
14. A. Bejan, Theory of heat transfer irreversible power plants, *Int. J. Heat Mass Transfer* **31,** 1211–1219 (1988).
15. A. Bejan, Power and refrigeration plants for minimum heat exchanger size, *J. Energy Res. Technol.* **115,** 148–150 (1993).
16. A. Bejan, D. W. Kearney and F. Kreith, Second law analysis and synthesis of solar collector systems, *J. Solar Energy Engng* **103,** 23–30 (1981).
17. J. V. C. Vargas, Combined heat transfer and thermodynamics problems with applications in refrigeration, Ph.D. Thesis, Duke University, Durham, NC (1994).
18. A. Bejan, Second law aspects of thermal energy conversion, *Int. Conf. on Comparative Assessments of Solar Power Technologies*, Jerusalem, February 14–18 (1994).